A Thermoresponsive Bubble-Generating Liposomal System for Triggering Localized Extracellular Drug Delivery

Ko-Jie Chen,[†] Hsiang-Fa Liang,[‡] Hsin-Lung Chen,[†] Yucai Wang,[⊥] Po-Yuan Cheng,[†] Hao-Li Liu,[§] Younan Xia,[⊥,*] and Hsing-Wen Sung[†,*]

[†]Department of Chemical Engineering and Institute of Biomedical Engineering, National Tsing Hua University, Hsinchu 30013, Taiwan, ROC, [‡]Biomedical Technology and Device Research Laboratories, Industrial Technology Research Institute, Hsinchu 30013, Taiwan, ROC, [⊥]The Wallace H. Coulter Department of Biomedical Engineering, Georgia Institute of Technology and Emory University, Atlanta, Georgia 30332, United States, and [§]Department of Electrical Engineering, Chang-Gung University, Taoyuan 33302, Taiwan, ROC

ABSTRACT The therapeutic effectiveness of chemotherapy is optimal only when tumor cells are subjected to a maximum drug exposure. To increase the intratumoral drug concentration and thus the efficacy of chemotherapy, a thermoresponsive bubble-generating liposomal system is proposed for triggering localized extracellular drug delivery. The key component of this liposomal formulation is the encapsulated ammonium bicarbonate (ABC), which is used to create the transmembrane gradient needed for a highly efficient encapsulation of doxorubicin (DOX). At an elevated temperature (42 °C), decomposition of ABC generates CO_2 bubbles, creating permeable defects in the lipid bilayer that rapidly release DOX and instantly increase the drug concentration locally. Because the generated CO_2 bubbles are hyperechogenic, they also enhance ultrasound imaging. Consequently, this new liposomal system encapsulated with ABC may also provide an ability to monitor a temperature-controlled drug delivery process.

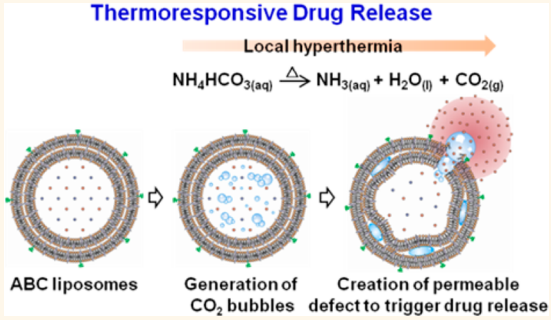

KEYWORDS: thermoresponsive liposome · triggered release · drug delivery · doxorubicin · chemotherapy

The PEGylated liposomal doxorubicin (DOX) or Doxil has been used for the treatment of a variety of cancers due to its prolonged circulation time, increased drug accumulation in solid tumors, and reduced acute cardiotoxicity relative to free DOX.[1−4] However, the slow (<5% in 24 h) and passive drug release from the Doxil formulation substantially limits its antitumor efficacy.[5,6] Therefore, a method capable of actively triggering DOX release is needed to increase its therapeutic efficacy on tumor cells. A lysolipid thermoresponsive liposomal formulation (ThermoDOX), which can be triggered to release DOX rapidly at elevated temperatures (40−42 °C), has proven to be more effective in reducing tumor volume in an animal model study.[7−9] Although ThermoDOX has great therapeutic potential, approximately 50% of its encapsulated DOX is released from the liposomal carrier within 1 h after intravenous administration.[10,11] Lysolipid dissociation from the liposomes, as induced and mediated by plasma proteins, is a suspected cause of their intravenous instability.[12,13]

In a recent study, we reported a new cationic liposomal system that contained ammonium bicarbonate (ABC, NH_4HCO_3), a raising agent commonly used in the food industry to generate gas bubbles in baked goods.[14] After endocytosis and intracellular trafficking to lysosomes, the ABC-containing liposomes could be thermally triggered to generate CO_2 bubbles, which then grew rapidly, collapsed violently, and ultimately led to transient cavitation. As a result, the lysosomal membranes were disrupted to spill proteases into the cytosol, causing cell necrosis.[15] These findings suggest that the ABC-containing liposomes can also be used as a new class of thermoresponsive carriers for the delivery of a drug into a locally heated tumor at a high dosage, thus minimizing the systemic cytotoxicity of the drug. This new system can also solve the problem

* Address correspondence to younan.xia@bme.gatech.edu, hwsung@che.nthu.edu.tw.

Received for review September 27, 2012 and accepted December 14, 2012.

Published online December 14, 2012
10.1021/nn304474j

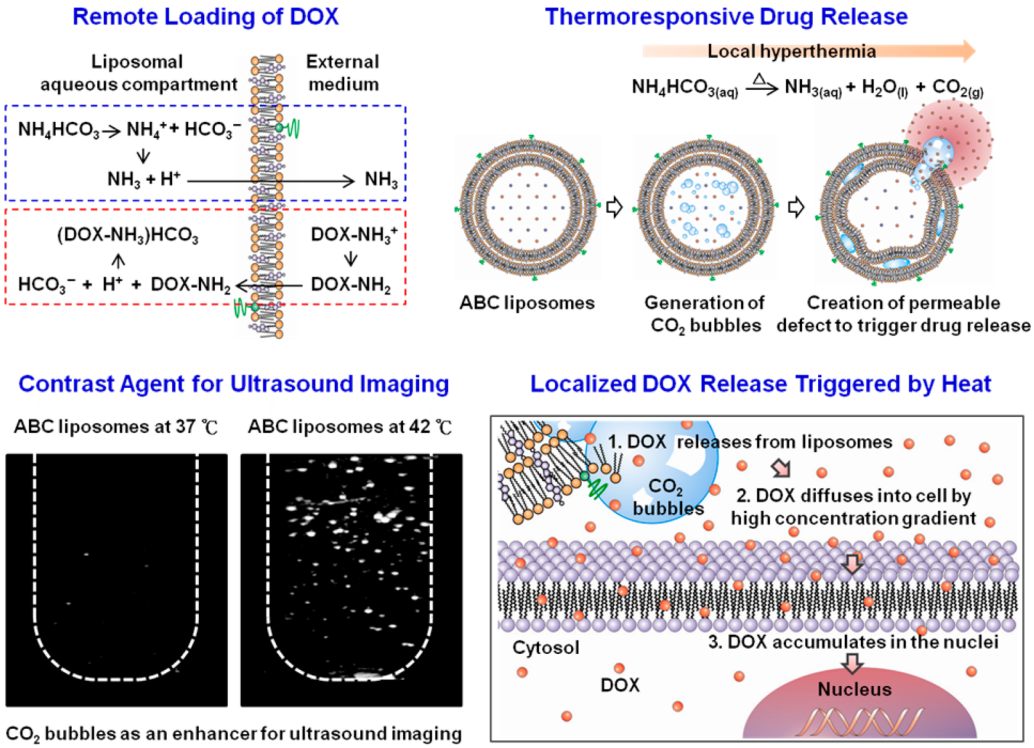

Figure 1. Schematic illustrations showing the structure and functions of the thermoresponsive, bubble-generating liposomes demonstrated in the present work and the mechanism of localized extracellular drug release as triggered by heat.

of intravenous instability associated with ThermoDOX. Figure 1 shows a schematic of the new liposomal system and how it works. The key component of this liposomal carrier is ABC, which can be readily incorporated into the aqueous compartment of liposomes to generate ABC liposomes when the lipids are hydrated to form a suspension. Rapid release of the drug from liposomes can be achieved by thermal stimulation.

A remote-loading technique can also be used to achieve highly efficient DOX encapsulation. After the unencapsulated ABC has been removed *via* dialysis, DOX is added to the liposome suspension at room temperature. Some of the encapsulated ammonium (NH_4^+) ions dissociated into protons (H^+) and ammonia (NH_3). The ammonia molecules rapidly cross the liposomal membrane and leaves free protons trapped in the liposomes because of their low membrane permeability. When the unprotonated DOX enters the proton-rich environment of the liposomal aqueous compartment by diffusion, it becomes protonated to generate a DOX-bicarbonate salt by reacting with bicarbonate (HCO_3^-). The DOX in the liposomal aqueous phase can eventually reach a concentration exceeding its solubility limit in water.[16−18] This technique can also be used to load amphipathic drugs (weak acids with acetate group or weak bases with ammonium group).[19]

Besides acting as an agent for remote-loading of DOX, the ABC encapsulated in liposomes can be used to trigger rapid drug release *via* mild hyperthermia. Upon heating to a temperature of 40 °C or above, ABC quickly decomposes to generate CO_2 bubbles,[20,21] creating permeable defects in the lipid bilayer and thereby swiftly releasing DOX. This mechanism offers a unique means to trigger localized extracellular drug release in a locally heated tumor, generating a high drug concentration gradient across the cell membrane. After diffusing into a cell and eventually entering the cell nucleus, the drug molecules bind strongly to nuclear DNA, causing the cell to die (Figure 1). Meanwhile, mild hyperthermia can also increase tumor perfusion and increase drug sensitivity in the cell.[22,23]

RESULTS AND DISCUSSION

Characteristics of the Test Liposomes. This study used the lipid film hydration technique, followed by sequential extrusion,[24,25] to prepare the test liposomes at room temperature with an aqueous solution containing saturated ABC (2.7 M, as determined by a titration method). A mixture of 1,2-dihexadecanoyl-*sn*-glycero-3-phosphocholine (DPPC), cholesterol, and 1,2-distearoyl-*sn*-glycero-3-phosphoethanolamine-*N*-(amino-(polyethylene glycol)-2000) (DSPE-PEG2000) at a mole ratio of 6.0:4.0:0.5 was used for the lipid formulation. The as-prepared liposomes had a melting temperature of 52.0 °C, as determined using a differential scanning calorimeter. Table 1 lists the amounts of DOX encapsulated in the ABC liposomes prepared at different drug/lipid ratios (by w/w). The liposomes formulated in the presence of aqueous ammonium sulfate

TABLE 1. Formulation Parameters of ABC and AS Liposomes Containing Doxorubicin (DOX); the Data Are Presented As Mean ± SD (n = 6)

liposomes	drug/lipid ratio (by w/w)[a]	diameter (nm)	polydispersity index	zeta potential (mv)	encapsulation efficiency (%)[b]	encapsulated DOX (mg)
ABC	0.02	150.4 ± 0.9	0.09 ± 0.02	−0.11 ± 0.01	90.5 ± 8.4	0.18 ± 0.02
ABC	0.05	150.5 ± 0.6	0.07 ± 0.01	−0.12 ± 0.01	96.2 ± 6.1	0.48 ± 0.03
ABC	0.10	150.9 ± 0.6	0.08 ± 0.01	−0.10 ± 0.01	93.9 ± 5.7	0.94 ± 0.06
AS	0.10	151.4 ± 0.4	0.07 ± 0.01	−0.11 ± 0.01	92.3 ± 6.7	0.92 ± 0.07

[a] Total lipid concentration: 10 mg/mL. [b] Drug encapsulation efficiency (%) was calculated using the formula: (weight of drug loaded ×100)/(total weight of drug added in the preparation).

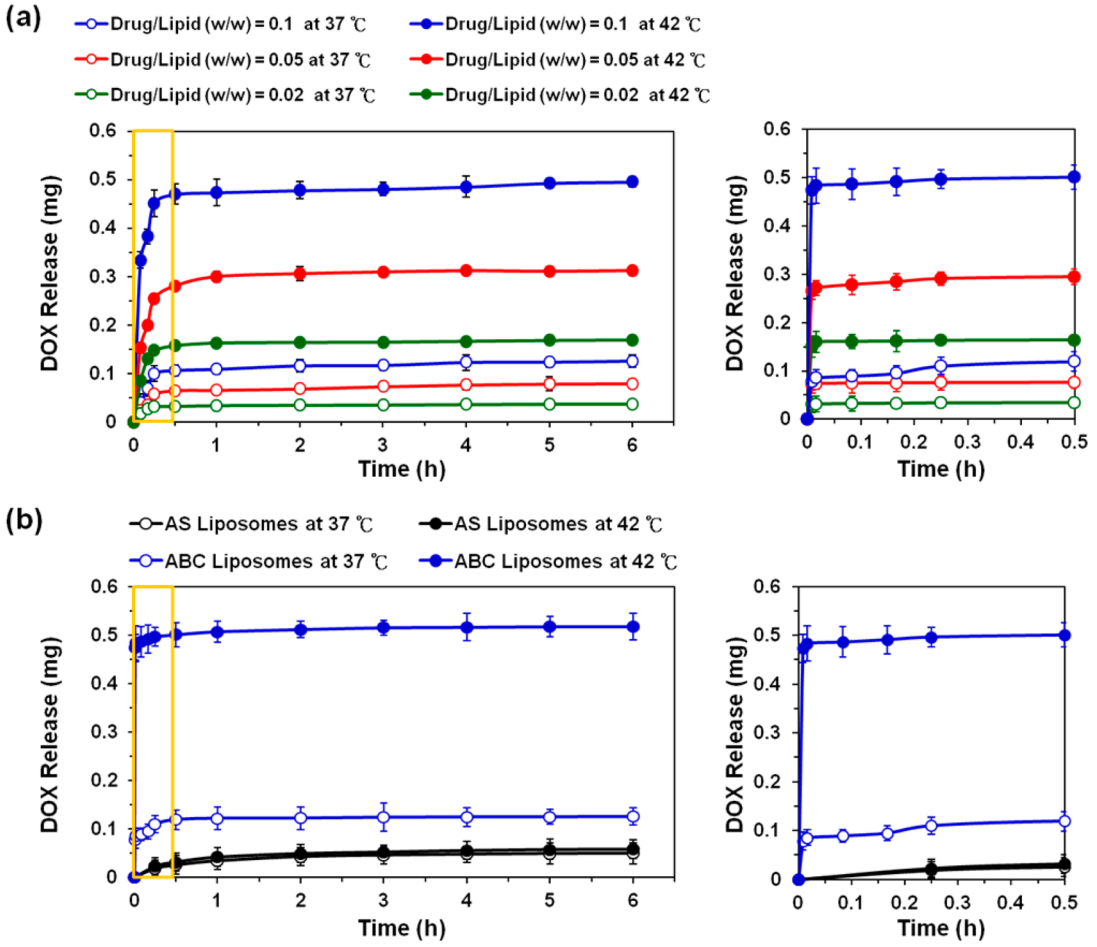

Figure 2. (a) Release profiles of DOX from the ABC liposomes prepared at different drug/lipid ratios and incubated in PBS at 37 or 42 °C (n = 6), respectively; (b) release profiles of DOX from the AS and ABC liposomes (drug/lipid ratio = 0.1) incubated in PBS at 37 and 42 °C (n = 6), respectively. A zoom-in plot of drug release in the first couple of minutes is also shown at the right-hand side in each figure.

(AS liposomes) were used as a control. We achieved efficient (>90%) and stable loading of DOX into the aqueous phase of the liposomes by taking advantage of the transmembrane gradient of AS or ABC. Typically, the DOX encapsulated in the liposomes was about 100-fold higher than its saturated concentration in water at room temperature. Dynamic light scattering (DLS) measurements indicate that the sizes and surface potentials of ABC and AS liposomes were comparable (P > 0.05, Table 1).

***In Vitro* Release Profiles.** Figure 2a shows the release profiles of DOX from the ABC liposomes that were prepared at different drug/lipid ratios and then incubated in phosphate buffered saline (PBS) at 37 and 42 °C, respectively. The original point in the x-axis corresponds to the beginning of heat triggering. Since the cell killing rate depends on the mass dose of a drug, the release profiles were presented as the mass of DOX released as a function of time. Among all studied groups, the ABC liposomes formulated at a drug/lipid ratio of 0.10 showed the highest DOX release at 42 °C.

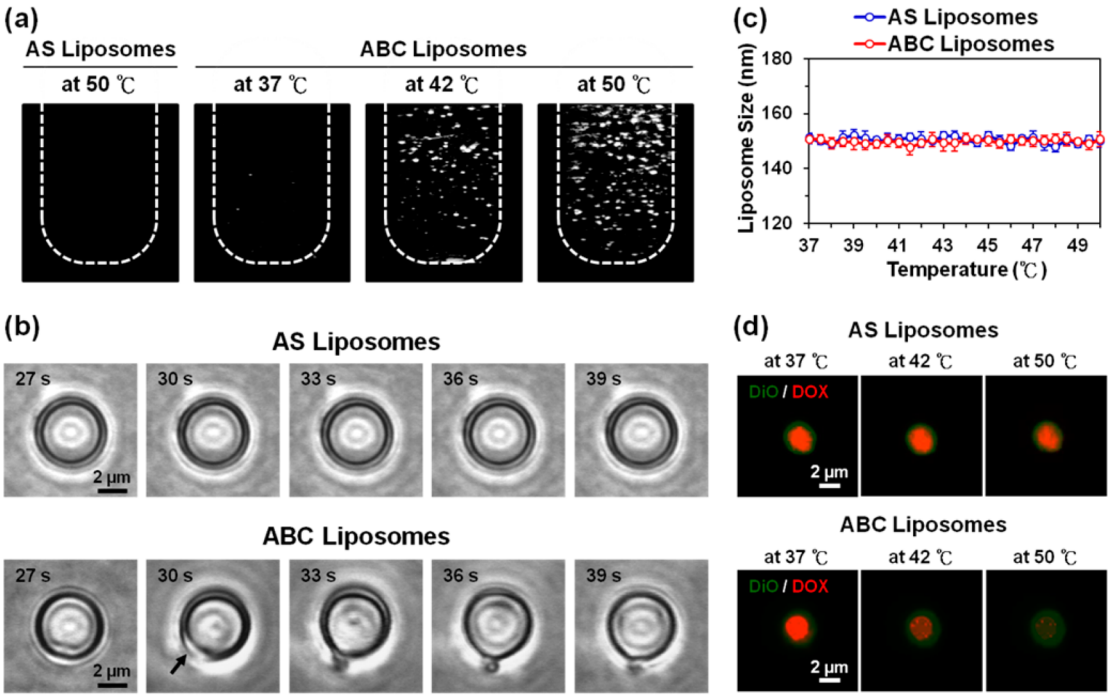

Figure 3. (a) Ultrasound images of the AS and ABC liposomes suspended in aqueous media and held at different temperatures; (b) CLSM images of AS and ABC liposomes following heating to a local temperature of 42 °C; (c) sizes of the AS and ABC liposomes in PBS at different temperatures ($n = 6$); and (d) fluorescence micrographs showing the changes in color of AS and ABC liposomes at different temperatures. In panels b and d, liposomes with relatively large diameters around 4 μm were used for the purpose of imaging.

Therefore, this specific formulation was used in the remaining experiments.

The drug release behaviors of the ABC liposomes were then compared with those of the AS liposomes. As shown in Figure 2b, the amounts of DOX released from the AS liposomes were minimal during the entire course of the study at both temperatures (0.06 mg or 6% of the originally encapsulated content), suggesting that the release of DOX from the AS liposomal carrier was rather slow and temperature independent due to the lack of a triggering mechanism.

Conversely, DOX release from the ABC liposomes was highly dependent upon the environmental temperature, a characteristic feature of thermoresponsive drug release. The extent of DOX released from the ABC liposomes at 37 °C was relatively low (approximately 0.1 mg or 10% of the initial content). When heated to 42 °C, however, a significant amount of the encapsulated DOX (0.5 mg or 50%) was released instantly (within 30 s). Additionally, the ABC formulation displayed a significantly improved stability in whole blood at 37 °C (approximately 85% retention of DOX in 1 h), as compared to the lysolipid temperature-sensitive liposomes (50% retention). These experimental results suggest that the ABC formulation is relatively stable at 37 °C and can retain the drug within the liposomes during blood circulation. The drug release will be extremely fast, however, when the carrier is locally heated, generating a high drug concentration gradient to facilitate diffusion of drug molecules into the tumor cells (Figure 1). It is worth pointing out that maximum therapeutic effects may only be achieved when tumor cells are subject to a maximum drug exposure.[26]

The Role of ABC in Triggering Drug Release. Heating causes ABC to decompose into water, ammonia, and CO_2 bubbles.[20,21] A kinetic analysis of the reaction suggested that the decomposition of aqueous ABC was a second order, irreversible reaction.[27] We evaluated the temperature sensitivity of ABC liposomes by their abilities to generate CO_2 bubbles when they were suspended in aqueous media and held at distinct environmental temperatures with their AS counterparts serving as a control. The test tubes containing the samples were immersed in a water-filled tank, and the formation of CO_2 bubbles was examined using an ultrasound imaging system.[15,28] Since the CO_2 bubbles are hyperechogenic, they act as an enhancer for ultrasound imaging.[29]

At all temperatures tested, the AS liposomes produced no bubbles (Figure 3a). Conversely, CO_2 bubbles appeared in the sample of ABC liposomes immediately after elevation of the environmental temperature and the amount of CO_2 bubbles observed in the test tube was in a temperature dependent manner. The higher the environmental temperature was that the ABC liposomes were subjected to, the more CO_2 bubbles would be generated. These observations indicate that the decomposition of ABC encapsulated in liposomes could enable immediate thermal activation of CO_2 bubble formation. Our titration analysis revealed that

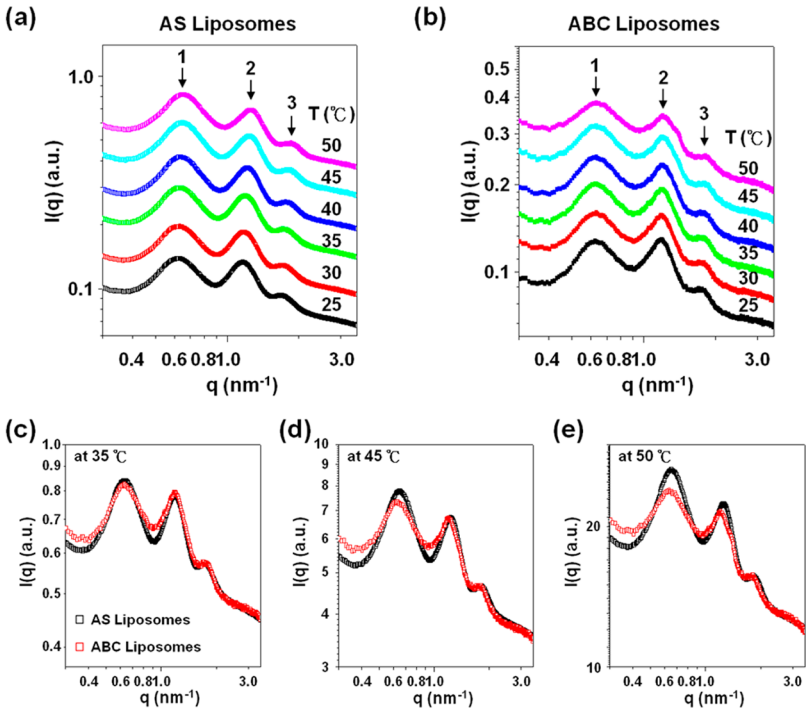

Figure 4. SAXS profiles of the (a) AS and (b) ABC liposome suspensions collected in a heating cycle. The SAXS profiles of AS and ABC liposomes at (c) 35 °C, (d) 45 °C, and (e) 50 °C.

the extents of ABC decomposition were approximately 20% and 40%, respectively, at 42 and 50 °C.

The process in which CO_2 bubbles were released from a liposome was further studied using ABC liposomes prepared as described above but without sequential extrusion. The liposomes (approximately 4 μm in diameter; to overcome the resolution limit of optical instruments) were examined under a confocal laser scanning microscope (CLSM) with their AS counterparts being used as a control. The camera system was operated at a speed of 20 frames per min. Figure 3b shows representative CLSM images of AS and ABC liposomes after the local temperature was increased to 42 °C. Throughout the course of the study, no gas bubbles were observed for the AS liposomes. In contrast, heating the ABC liposomes generated CO_2 bubbles in their aqueous compartment. Once their internal pressure reached a certain level, the gas bubbles permeated the membrane and formed a transient pore (as indicated by the arrow in the second frame taken at 30 s after heating), through which the CO_2 bubbles escaped and then detached (at 39 s) from the liposomes. Thereafter, the lipid bilayer relaxed and resumed its initial impermeable state. This process occurred within only 40 s. Thus, the sizes of the ABC liposomes were apparently invariant at all temperatures tested (Figure 3c). These experimental results confirm that the CO_2 bubbles from the decomposition of ABC can convert liposome membranes into a permeable structure to enable drug release at the very beginning of heating.

The DOX release from test liposomes was demonstrated by labeling the liposomes with DiO (3,3′-dioctadecyloxacarbocyanine, perchlorate), a lipophilic fluorescent dye. At all temperatures, the consistently orange color (superposition of green DiO and red DOX) of the AS liposome indicate that the DOX release from the carrier was minimal (Figure 3d). Conversely, the color of the ABC liposome changed from orange (at 37 °C) to yellow (at 42 °C) to green (at 50 °C) as temperature increased due to release of DOX through the permeable defects as described above.

Structural analyses of the test liposomes were also performed by small-angle X-ray scattering (SAXS) at different temperatures. Figure 4a displays the SAXS profiles of the AS liposome suspension collected during a heating cycle. A series of scattering peaks with an integral position ratio of 1:2:3 were observed, indicating that the as-prepared liposomes were multilamellar vesicles. The interlamellar distance (*i.e.*, the sum of the thickness of a hydrophobic layer and a hydrophilic layer) calculated from the primary peak position (qm) *via* $d = 2\pi/qm$ was 10 nm. The correlation length of the lamellar stacking in the vesicle estimated from the full width at half height ($/\Delta qm$) of the primary peak *via* $D = 2\pi/\Delta qm$ was about 25 nm; therefore, there were about 2−3 lamella involved in the formation of a vesicle. The scattering pattern in terms of the positions and breadths of the peaks remained essentially changed with increasing temperature, implying that the vesicles were structurally stable up to at least 50 °C.

Figure 4b shows the temperature-dependent SAXS profiles of the ABC liposomes. Again, the integral position ratios of the observed scattering peaks indicate that the prepared liposomes were multilamellar vesicles with interlamellar distances similar to those obtained for the AS liposomes. Indeed, the SAXS profile of ABC liposomes superposed fairly well with that of the AS counterparts when the temperature was below 40 °C (Figure 4c). This data attests that the incorporation of ABC into liposomes did not perturb the membrane structures significantly. However, at local temperatures exceeding 40 °C, significant broadening and intensity reduction were observed for the scattering peaks (Figure 4d,e), suggesting that the structures of the membrane became more disordered. The observed structural perturbation could be attributed to CO_2 bubble formation in the liposomes at elevated temperatures.

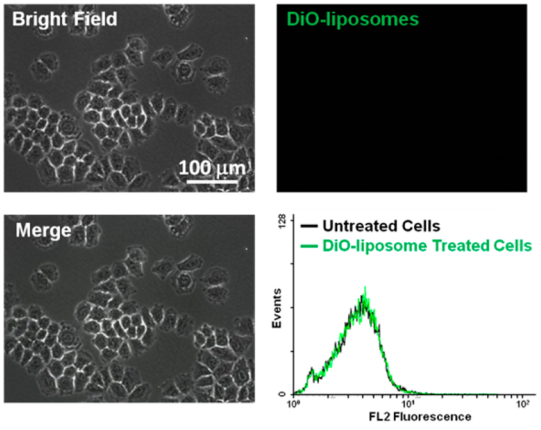

Figure 5. Fluorescence microscopy and flow cytometry investigation of the cellular uptake efficiency of DiO-labeled liposomes by H460 cells after 2 h incubation.

The release of relatively large bubbles formed may destabilize the liposomes, hence causing a decrease for the intensity of the peak associated with the multilamellar vesicles. On the other hand, some of the CO_2 bubbles of nanoscale in size might be trapped in the membranes, so as to create some defects and distort the original regular stacking of the membrane bilayers (see Figure 1). The structural perturbation revealed by SAXS is in agreement with the proposed mechanism of the formation and release of CO_2 bubbles at elevated temperatures.

Extracellular Release of DOX and Its Intracellular Accumulation. As shown by flow cytometry and fluorescence microscopy, no intracellular fluorescence was observed (Figure 5) after H460 cells (human lung nonsmall carcinoma cell line) had been incubated in a medium containing DiO-labeled liposomes for 2 h. This result suggests that the ABC liposomes containing DSPE-PEG2000 were unable to enter the tumor cells. Adding PEG-lipids prolongs the circulation lifetimes of liposomes but inhibits their cellular uptake.[30,31] Therefore, drug release from ABC liposomes can be triggered only extracellularly. Extracellular drug release at the tumor site appears preferable since it allows for diffusion of the drug within the solid tumors and also enables the

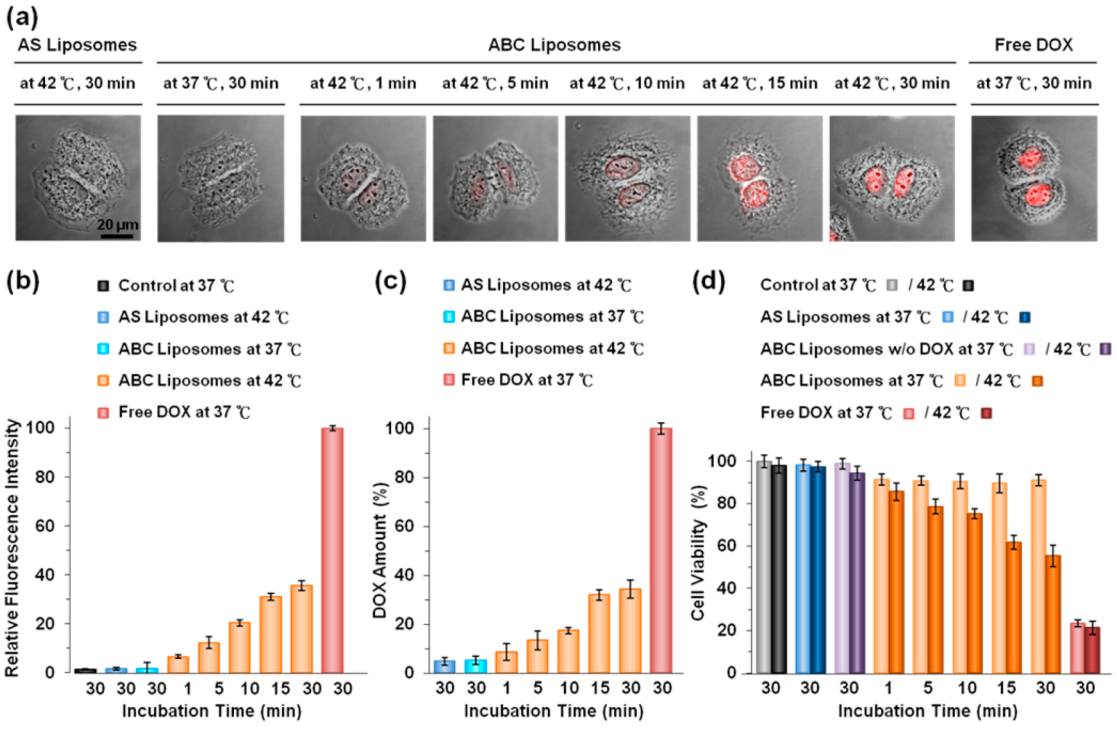

Figure 6. (a) CLSM images and results of (b) flow-cytometry and (c) direct fluorometry measurements of the intracellular accumulation of DOX in H460 cells treated with AS liposomes, ABC liposomes, or free DOX (20 μM of DOX in each studied group) at distinct environmental temperatures and (d) their cell viability, as determined by the MTT assay.

drug to reach tumor cells that do not internalize the drug carriers.[32]

The kinetics of DOX accumulation in cells was characterized by visualizing the intracellular localization of DOX in H460 cells. No DOX (with red fluorescence) accumulation occurred in the nuclei of cells incubated with the AS liposomes for 30 min (Figure 6a). In the group treated with the ABC liposomes, no apparent intracellular DOX accumulation was observed at 37 °C. Conversely, at 5 min after heating to 42 °C, weak red fluorescence (indicative of DOX) appeared near the cell nuclei; over time, the DOX accumulation in the cell nuclei gradually increased.

The above observations were also confirmed by our quantitative flow cytometry and direct fluorometry measurements (Figure 6b,c). Flow cytometry analysis indicates that after initial drug exposure, accumulation of free DOX in H460 cells was clearly noted. Accumulation of DOX in cells treated with the ABC liposomes increased constantly with the incubation time. Similar results were obtained by using quantitative fluorometry of DOX from cellular lysates with a fluorescence spectrometer, a method that is relatively unaffected by quenching artifacts.[33]

Transport of DOX into the cell nuclei, where it has cytotoxic effects, is an important process. Figure 6d summarizes the results of cell viability after the cells had been incubated with the AS and ABC liposomes, respectively, with cells receiving no liposomes as a control. Similar to the control group, no apparent cytotoxicity was observed for the cells treated with the AS liposomes at 37 and 42 °C for 30 min ($P > 0.05$); this finding suggests that the amount of DOX released from the AS liposomes was minimal and could not cause a significant cell death, due to their slow and passive drug diffusion process. For the group treated with the ABC liposomes at 37 °C, most cells were viable; however, when raising the local temperature to 42 °C, the cell viability declined markedly with time according to the amount of DOX accumulated in the cell nuclei ($P < 0.05$, $n = 6$). In this case, the cell death was believed to arise from the formation of CO_2 bubbles during the heating of ABC liposomes, leading to the structural perturbation of their lipid membranes, promptly releasing DOX, and ultimately causing the death of cells.

CONCLUSIONS

In summary, this study successfully demonstrated a thermoresponsive, bubble-generating liposomal system with high capacity for DOX encapsulation. The system also enables heat-triggered release of DOX for localized extracellular drug delivery. This novel carrier for drug delivery can be used for controlled release of drugs in a locally heated tumor or as an ultrasound reporter for probing the status of vehicles after heat triggering.

EXPERIMENTAL SECTION

Materials. The DPPC and DSPE-PEG2000 were purchased from Avanti Polar Lipids (Alabaster, AL, USA), while DOX was obtained from Fisher Scientific (Waltham, MA, USA). The AS, ABC, and cholesterol were ordered from Sigma-Aldrich (St. Louis, MO, USA). All other chemicals and reagents used were of analytical grade.

Liposome Preparation. Liposome colloidal suspensions were prepared by dissolving the lipid mixture in chloroform. The organic solvent was removed with a rotavapor to generate a thin lipid film (10 mg) on the glass vial. The lipid film was then hydrated with an aqueous AS (350 mM) or ABC (2.7 M) solution *via* sonication at room temperature and followed by sequential extrusions through 800, 400, 200, and 100 nm polycarbonate filters (six times each) at room temperature. The recovery rate of the lipid following multiple extrusions was approximately 90%, as determined by the lipid phosphate assay. The free AS or ABC was removed by dialysis against a 10 wt % sucrose solution with 5 mM NaCl. Subsequently, DOX was mixed to the liposome suspensions at distinct drug/lipid ratios and maintained at room temperature for 24 h. Finally, the liposomes were passed through another G-50 column (GE Healthcare, Buckinghashire, UK) to remove the unencapsulated DOX.

Characterization of Test Liposomes. The encapsulated DOX concentration was measured using fluorescence measurements (Spex FluoroMax-3, Horiba Jobin Yvon, Edison, NJ, USA) after destruction of the liposomes with Triton X-100. The mean particle size and zeta potential of the liposomes was evaluated by DLS (Zetasizer 3000HS, Malvern Instruments Ltd., Worcestershire, UK); also, the polydispersity index, a value indicating the size distribution of the liposomes was determined.

Release of DOX from Test Liposomes. An aliquot of dispersed DOX-loaded liposomes was added to a quartz cell; fluorescence intensity of the solution was monitored with a fluorescence spectrometer at 37 and 42 °C over time.

Ultrasound Imaging. The thermoresponsive characteristics of the ABC liposomes were evaluated by examining the generation of CO_2 bubbles in a test tube containing the particles in PBS (pH 7.4) at 37, 42, and 50 °C; the AS liposomes were used as a control. The test tube was immersed in a water-filled tank, and an ultrasound imaging system with a 7 MHz linearray transducer (Z-one, Zonare, Mountain View, CA, USA) was employed to visualize the CO_2 bubbles. Consecutive ultrasonic B-mode images were recorded with a computer.

SAXS Measurements. The structures of the liposomes were probed by SAXS at different temperatures. The aqueous suspensions of the liposomes were directly introduced into the sample cell comprising two Kapton windows. The SAXS experiments were performed at the Endstation BL23A1 of the National Synchrotron Radiation Research Center (NSRRC), Taiwan. The energy of X-ray source and sample-to-detector distance were 14 keV and 2259 mm, respectively. The scattering signals were collected by a MarCCD detector of 512 × 512 pixel resolution. The scattering intensity profile was output as the plot of the scattering intensity $I(q)$ *versus* the scattering vector, $q = (4\pi/\lambda)\sin(\theta/2)$ (θ = scattering angle), after corrections for sample transmission, empty cell transmission, empty cell scattering, and the detector sensitivity.

Internalization of ABC Liposomes. The ability of cellular internalization of the ABC liposomes was analyzed by fluorescence microscopy (Axio Observer, Carl Zeiss, Jena, Germany) and flow cytometry (Beckman Coulter, Fullerton, CA, USA). H460 cells were treated with DiO-labeled ABC liposomes in the serum-free medium; after incubation for 2 h, test samples were aspirated. Cells were then washed twice with the prewarmed PBS before they were fixed in 4% paraformaldehyde.

Intracellular Accumulation of DOX. To monitor the DOX accumulation intracellularly, H460 cells were treated with test liposomes in the serum-free medium. After incubation, the cells were washed twice with prewarmed PBS and then fixed in 4% paraformaldehyde. The intracellular accumulation of DOX was qualitatively examined using CLSM (TCS SL, Leica, Germany) and quantitatively determined by flow cytometery.

Intracellular DOX accumulation was also evaluated using a fluorimetric assay as described elsewhere.[34] After treatment, the cells were harvested and cell lysates were prepared. DOX concentrations in the cell lysates were then measured with a microplate fluorometer (SpectraMax Gemini XS, Molecular Devices, Sunnyvale, CA, USA) at an excitation wavelength of 485 nm and an emission wavelength of 560 nm. To adjust for background fluorescence from the cellular components, DOX standardization curves were also prepared using cell lysates. In this case, untreated cells were lysed with 1% Triton X-100 in PBS containing DOX at known concentrations.

Cell Viability Assay. H460 cells were cultured with test liposomes for varying durations. After treatment, the samples were aspirated, and cells were incubated in a medium containing 1 mg/mL MTT reagent for 4 h. A 1 mL quantity of DMSO was then added. Optical density readings were obtained with a multiwell scanning spectrophotometer.

Statistical Analysis. Two groups were compared by the one-tailed Student's *t*-test using statistical software (SPSS, Chicago, IL, USA). Data are presented as mean ± SD. A difference of $P < 0.05$ was considered statistically significant.

Conflict of Interest: The authors declare no competing financial interest.

Acknowledgment. This work was supported by a grant from the National Science Council (101-2120-M-007-015-CC1), Taiwan (ROC).

REFERENCES AND NOTES

1. Barenholz, Y. Doxil— The First FDA-Approved Nano-Drug: Lessons Learned. *J. Controlled Release* **2012**, *160*, 117–134.
2. Yang, F.; Jin, C.; Jiang, Y.; Li, J.; Di, Y.; Ni, Q.; Fu, D. Liposome Based Delivery Systems in Pancreatic Cancer Treatment: From Bench to Bedside. *Cancer Treat. Rev.* **2011**, *37*, 633–642.
3. Elbayoumi, T. A.; Torchilin, V. P. Tumor-Targeted Nanomedicines: Enhanced Antitumor Efficacy *in Vivo* of Doxorubicin-Loaded, Long-Circulating Liposomes Modified with Cancer-Specific Monoclonal Antibody. *Clin. Cancer Res.* **2009**, *15*, 1973–1980.
4. Pornpattananangkul, D.; Olson, S.; Aryal, S.; Sartor, M.; Huang, C. M.; Vecchio, K.; Zhang, L. Stimuli-Responsive Liposome Fusion Mediated by Gold Nanoparticles. *ACS Nano* **2010**, *4*, 1935–1942.
5. Tagami, T.; Ernsting, M. J.; Li, S. D. Optimization of a Novel and Improved Thermosensitive Liposome Formulated with DPPC and a Brij Surfactant Using a Robust *in Vitro* System. *J. Controlled Release* **2011**, *154*, 290–297.
6. Allen, T. M.; Cullis, P. R. Drug Delivery Systems: Entering the Mainstream. *Science* **2004**, *303*, 1818–1822.
7. Chang, H. I.; Yeh, M. K. Clinical Development of Liposome-Based Drugs: Formulation, Characterization, and Therapeutic Efficacy. *Int. J. Nanomed.* **2012**, *7*, 49–60.
8. Dromi, S.; Frenkel, V.; Luk, A.; Traughber, B.; Angstadt, M.; Bur, M.; Poff, J.; Xie, J.; Libutti, S. K.; Li, K. C.; *et al.* Pulsed-High Intensity Focused Ultrasound and Low Temperature-Sensitive Liposomes for Enhanced Targeted Drug Delivery and Antitumor Effect. *Clin. Cancer Res.* **2007**, *13*, 2722–2727.
9. Shenoi, M. M.; Shah, N. B.; Griffin, R. J.; Vercellotti, G. M.; Bischof, J. C. Nanoparticle Pre-conditioning for Enhanced Thermal Therapies in Cancer. *Nanomedicine* **2011**, *6*, 545–563.
10. Chiu, G. N.; Abraham, S. A.; Ickenstein, L. M.; Ng, R.; Karlsson, G.; Edwards, K.; Wasan, E. K.; Bally, M. B. Encapsulation of Doxorubicin into Thermosensitive Liposomes *via* Complexation with the Transition Metal Manganese. *J. Controlled Release* **2005**, *104*, 271–288.
11. Banno, B.; Ickenstein, L. M.; Chiu, G. N.; Bally, M. B.; Thewalt, J.; Brief, E.; Wasan, E. K. *J.* The Functional Roles of Poly-(ethylene glycol)-Lipid and Lysolipid in the Drug Retention and Release from Lysolipid-Containing Thermosensitive Liposomes *in Vitro* and *in Vivo*. *Pharm. Sci.* **2010**, *99*, 2295–2308.
12. Cullis, P. R.; Chonn, A.; Semple, S. C. Interactions of Liposomes and Lipid-Based Carrier Systems with Blood Proteins: Relation to Clearance Behaviour *in Vivo*. *Adv. Drug Delivery Rev.* **1998**, *32*, 3–17.
13. Mills, J. K.; Needham, D. Lysolipid Incorporation in Dipalmitoylphosphatidylcholine Bilayer Membranes qEnhances the Ion Permeability and Drug Release Rates at the Membrane Phase Transition. *Biochim. Biophys. Acta* **2005**, *1716*, 77–96.
14. Min, B.; Bae, I. Y.; Lee, H. G.; Yoo, S. H.; Lee, S. Utilization of Pectin-Enriched Materials from Apple Pomace as a Fat Replacer in a Model Food System. *Bioresour. Technol.* **2010**, *101*, 5414–5418.
15. Chung, M. F.; Chen, K. J.; Liang, H. F.; Liao, Z. X.; Chia, W. T.; Xia, Y.; Sung, H. W. A New Liposomal System Capable of Generating CO_2 Bubbles to Induce Transient Cavitation, Lysosomal Rupturing, and Cell Necrosis. *Angew. Chem., Int. Ed.* **2012**, *51*, 10089–10093.
16. Cern, A.; Golbraikh, A.; Sedykh, A.; Tropsha, A.; Barenholz, Y.; Goldblum, A. Quantitative Structure-Property Relationship Modeling of Remote Liposome Loading of Drugs. *J. Controlled Release* **2012**, *160*, 147–157.
17. Tagami, T.; May, J. P.; Ernsting, M. J.; Li, S. D. A Thermosensitive Liposome Prepared with a Cu^{2+} Gradient Demonstrates Improved Pharmacokinetics, Drug Delivery and Antitumor Efficacy. *J. Controlled Release* **2012**, *161*, 142–149.
18. Bolotin, E. M.; Cohen, R.; Bar, L.; Emanuel, N.; Ninio, S.; Barenholz, Y.; Lasic, D. D. Ammonium Sulfate Gradients for Efficient and Stable Remote Loading of Amphipathic Weak Bases into Liposomes and Ligandoliposomes. *J. Liposome Res.* **1994**, *4*, 455–479.
19. Cern, A.; Golbraikh, A.; Sedykh, A.; Tropsha, A.; Barenholz, Y.; Goldblumb, A. Quantitative Structure—Property Relationship Modeling of Remote Liposome Loading Of Drugs. *J. Controlled Release* **2012**, *160*, 147–157.
20. Boddien, A.; Gärtner, F.; Federsel, C.; Sponholz, P.; Mellmann, D.; Jackstell, R.; Junge, H.; Beller, M. CO_2-"Neutral" Hydrogen Storage Based on Bicarbonates and Formates. *Angew. Chem., Int. Ed.* **2011**, *50*, 6411–6414.
21. Yang, Y.; Bajaj, N.; Xu, P.; Ohn, K.; Tsifansky, M. D.; Yeo, Y. Development of Highly Porous Large PLGA Microparticles for Pulmonary Drug Delivery. *Biomaterials* **2009**, *30*, 1947–1953.
22. Eisenbrey, J. R.; Burstein, O. M.; Kambhampati, R.; Forsberg, F.; Liu, J. B.; Wheatley, M. A. Development and Optimization of a Doxorubicin Loaded Poly(lactic acid) Contrast Agent for Ultrasound Directed Drug Delivery. *J. Controlled Release* **2010**, *143*, 38–44.
23. Riehemann, K.; Schneider, S. W.; Luger, T. A.; Godin, B.; Ferrari, M.; Fuchs, H. Nanomedicine—Challenge and Perspectives. *Angew. Chem., Int. Ed.* **2009**, *48*, 872–897.
24. Soussan, E.; Cassel, S.; Blanzat, M.; Rico-Lattes, I. Drug Delivery by Soft Matter: Matrix and Vesicular Carriers. *Angew. Chem., Int. Ed.* **2009**, *48*, 274–288.
25. Boyer, C.; Zasadzinski, J. A. Multiple Lipid Compartments Slow Vesicle Contents Release in Lipases and Serum. *ACS Nano* **2007**, *1*, 176–182.
26. Allen, T. M. Ligand-Targeted Therapeutics in Anticancer Therapy. *Nat. Rev. Cancer* **2002**, *2*, 750–763.
27. Nowak, P.; Skrzypek, J. The Kinetics of Chemical Decomposition of Ammonium Bicarbonate and Carbonate in Aqueous Solutions. *Chem. Eng. Sci.* **1989**, *44*, 2375–2376.
28. Ke, C. J.; Su, T. Y.; Chen, H. L.; Liu, H. L.; Chiang, W. L.; Chu, P. C.; Xia, Y.; Sung, H. W. Smart Multifunctional Hollow Microspheres for the Quick Release of Drugs in Intracellular Lysosomal Compartments. *Angew. Chem., Int. Ed.* **2011**, *50*, 8086–8089.
29. Kang, E.; Min, H. S.; Lee, J.; Han, M. H.; Ahn, H. J.; Yoon, I. C.; Choi, K.; Kim, K.; Park, K.; Kwon, I. C. Nanobubbles from

Gas-Generating Polymeric Nanoparticles: Ultrasound Imaging of Living Subjects. *Angew. Chem., Int. Ed.* **2010**, *49*, 524–528.
30. Yamada, A.; Taniguchi, Y.; Kawano, K.; Honda, T.; Hattori, Y.; Maitani, Y. Design of Folate-Linked Liposomal Doxorubicin to Its Antitumor Effect in Mice. *Clin. Cancer Res.* **2008**, *14*, 8161–8168.
31. Gary, D. J.; Lee, H.; Sharma, R.; Lee, J. S.; Kim, Y.; Cui, Z. Y.; Jia, D.; Bowman, V. D.; Chipman, P. R.; Wan, L.; *et al*. The Influence of Nano-Carrier Architecture on *in Vitro* siRNA Delivery Performance and *in Vivo* Biodistribution: Polyplexes *vs* Micelleplexes. *ACS Nano* **2011**, *5*, 3493–3505.
32. McNeeley, K. M.; Karathanasis, E.; Annapragada, A. V.; Bellamkonda, R. V. Masking and Triggered Unmasking of Targeting Ligands on Nanocarriers to Improve Drug Delivery to Brain Tumors. *Biomaterials* **2009**, *30*, 3986–3995.
33. Riganti, C.; Miraglia, E.; Viarisio, D.; Costamagna, C.; Pescarmona, G.; Ghigo, D.; Bosia, A. Nitric Oxide Reverts the Resistance to Doxorubicin in Human Colon Cancer Cells by Inhibiting the Drug Efflux. *Cancer Res.* **2005**, *65*, 516–525.